Tungsten oxide thin film for room temperature nitrogen dioxide gas sensing.

Thokozani Mpanza[1], *Ceboliyazakha L.* Ndlangamandla[1] , Balla D. Ngom[1,2], *Steven S.* Nkosi[1], *Thulani P.* Jili[1], *Charles T.* Thethwayo[1], *Puleng N.* Biyela[1], *Ntokozo G.* Cebekhulu[1], *Prince S.* Mkwae[1], and *Sunday A.* Ogundipe[1]

[1]Department of Physics and Engineering: University of Zululand Private Bag X1001 KwaDlangezwa 3886, South Africa.

[2]Laboratoire de Photonique, d'Energie et de Nanofabrication, Faculté des Sciences et Techniques, Université Cheikh Anta Diop de Dakar (UCAD) B.P. 5005 Dakar-Fann Dakar, Senegal.

ABSTRACT. Tungsten oxide (WO_3) thin films for gas sensing have been successfully deposited using reactive direct current (DC) magnetron sputtering at different deposition temperatures (300 ºC, 400 ºC and 500 ºC). The structural, morphological properties, thickness and composition have been investigated using X-ray diffraction (XRD), scanning electron microscopy (SEM) and Rutherford backscattering spectrometry (RBS) techniques. To investigate the effect of deposition temperature on the gas sensing properties of deposited thin films on alumina substrates, was conducted using the Kenosistec gas sensing unit. WO_3 thin film deposited at 500 ºC exhibited a higher response when sensing Nitrogen dioxide (NO_2) at room temperature as compared to the thin films prepared at 300 ºC and 400 ºC, respectively. However, as deposited WO_3 thin films exhibited low sensitivity when sensing reducing gases such as hydrogen (H_2) and ammonia (NH_3), which was an indication of good selectivity properties of WO_3 related sensors.

Keywords: Tungsten Oxide, DC Reactive Sputtering, Thin Films, Nitrogen Dioxide, Gas Sensing

1. Introduction

There is a growing demand of metal oxide thin films for numerous important technological applications such as gas sensing, solar cells, solar absorbers, etc. The fast-growing industries and increase in exhaust emissions of gases from industries has put a large demand on the sensitive and selective detection of hazardous gases for environmental pollution monitoring, process control and safety for human health [1,2,3]. This has attributed to the fabrication of gas sensor devices [1,2,3,4,5]. NO_2 is one of the most potentially toxic gas which can lead to respiratory problems to humans. This gas leads to the formation of acid rains when excreted to air in its high concentrations above 0.65 ppm [1]. Therefore, the ability to accurately monitor or detect NO_2 concentrations in air is very crucial. A variety of metal oxide semiconductor nanostructures, such as ZnO [6], NiO-Nb_2O_5 [7], SnO [8], CuO [9], and VO_2 [10] and WO_3 [1] have been extensively investigated as gas sensing materials, however their responses towards NO_2 detection at room

© The Authors, published by EDP Sciences. This is an open access article distributed under the terms of the Creative Commons Attribution License 4.0 (http://creativecommons.org/licenses/by/4.0/).

temperature is still a challenge. Many previously reported metal oxide gas sensors are unable to detect NO_2 gas at low temperatures, hence an elevated temperatures e.g., 250 ºC was used when detecting NO_2. This is not good since high temperatures has resulted in high power consumption, which also reducing the gas sensor response of. The high concentration of NO_2 gas has been used previously when detecting NO_2, however a gas sensor that will detect and monitor NO_2 gas at room temperature and at low concentration is still needed to be fabricated since it is important to also detect NO_2 gas at low concentration. WO_3 is a promising material for detection of NO_2 [11]. Therefore, in this study WO_3 was prepare using different deposition temperatures (300, 400, and 500 ºC) to achieve different structures of WO_3 which play an important role in its gas sensing. Tungsten oxide nanostructures prepared by various methods are good candidates for detecting NO_2 because of their high crystallinity and large specific surface areas [1,11,12]. However, WO_3 based sensors require high operating temperatures (above 200 ºC) during gas detection because of high activation energy of reaction with gas molecules [12,13]. The high operating temperature during gas sensing is unfavorable for low power consumption and device integration [1]. Various attempt to reduce the operating temperature of WO_3 nanostructures based sensors such as WO_3 combine with other materials to form heterostructures or composite sensors have been performed [1,12]. Tungsten oxide (WO_3) is an n-type metal oxide semiconducting material with a band gap of about 2.7 eV [3]. WO_3 is considered to be a highly promising material for a broad range of applications such as in electronic devices, super-capacitors, optical aspects, gas sensors, solar energy, photocatalyst and biosensors [4,5,6,14,15,16,17]. This is because of its unique structural and physical properties, non-toxicity, and high chemical stability [4,5,6,14,15]. WO_3 exhibit various phases at temperature for example, it is tetragonal at temperatures above 740 ºC, orthorhombic between 330 to 740 ºC, monoclinic in the range of 17 ºC to 330 ºC and triclinic between -50 ºC and 17 ºC [5,6,14,15,16]. The most common structure of WO_3 is monoclinic [5]. Some previous studies have reported that n-type metal oxide nanostructures (e.g. WO_3) are promising materials for gas sensing since they have good electrical properties and excellent stability in various environments [6-15]. In this work, WO_3 thin films was deposited using DC magnetron sputtering for room temperature gas sensing of NO_2 gas. Different deposition temperatures was used to obtain different morphological structures which results in different gas sensing performance, this was done for the purpose of achieving a suitable WO_3 based sensor which is highly sensitive to low concentration of NO_2 and at room temperature. The DC sputtering deposition technique was used because of its fast deposition rate and good adhesion of clean, thin films on the substrates having no unwanted impurities [18].

2. Experimental procedure

2.1 Sample preparation

WO_3 thin films were synthesized on alumina substrates using a DC reactive magnetron sputtering technique. The 99.9% pure Tungsten target as purchased from AJA was sputtered at a pressure of 3×10^{-3} Torr for 50 minutes. Optimum deposition conditions for WO_3 thin films were reached through by varying the deposition power between 100 W to 200 W in steps of 50 W and the oxygen flow between 2 to 8 sccm.

RBS and XRD characterizations techniques revealed that the best deposition parameters to obtain well crystalline stoichiometric WO_3 thin films with high purity are a deposition power of 150W, an argon gas flow rate of 8 sccm and oxygen gas flow rate of 6 sccm, at a deposition pressure of $3x10^{-3}$ Torr for a deposition time of 50 minutes. These optimized deposition parameters were then used to synthesize different samples of WO_3 by varying the deposition temperature between 300ºC to 500ºC. Subsequent in attaining WO_3 thin films at 300ºC, 400ºC and 500ºC.

3. Results and discussion

Figure 1 (a-c) shows the images of SEM surface morphologies of WO_3 thin films that were deposited on silicon substrates using DC reactive magnetron sputtering at different deposition temperatures. Figure 1 (a), (b) and (c) are surface morphologies of WO_3 films prepared at 300, 400 and 500 ℃ respectively. During the deposition of WO_3 films, all other parameters were kept constant except the deposition temperature which was varied (300, 400 and 500 ℃). Therefore, it can be concluded that as the deposition temperature changes the surface morphology of WO_3 film also changes. At a deposition temperature of 300 ℃, the WO_3 surface morphology exhibits an evenly distributed small nano-spherical particles. At 400 ℃, a morphological structure of none-spherical granules was observed, and WO_3 prepared at 500 ℃, exhibited the morphology of cornflakes like in shape. The different morphological structures of WO_3 samples resulted on different gas sensing responses of WO_3, as it is explained under gas sensing results section of this document.

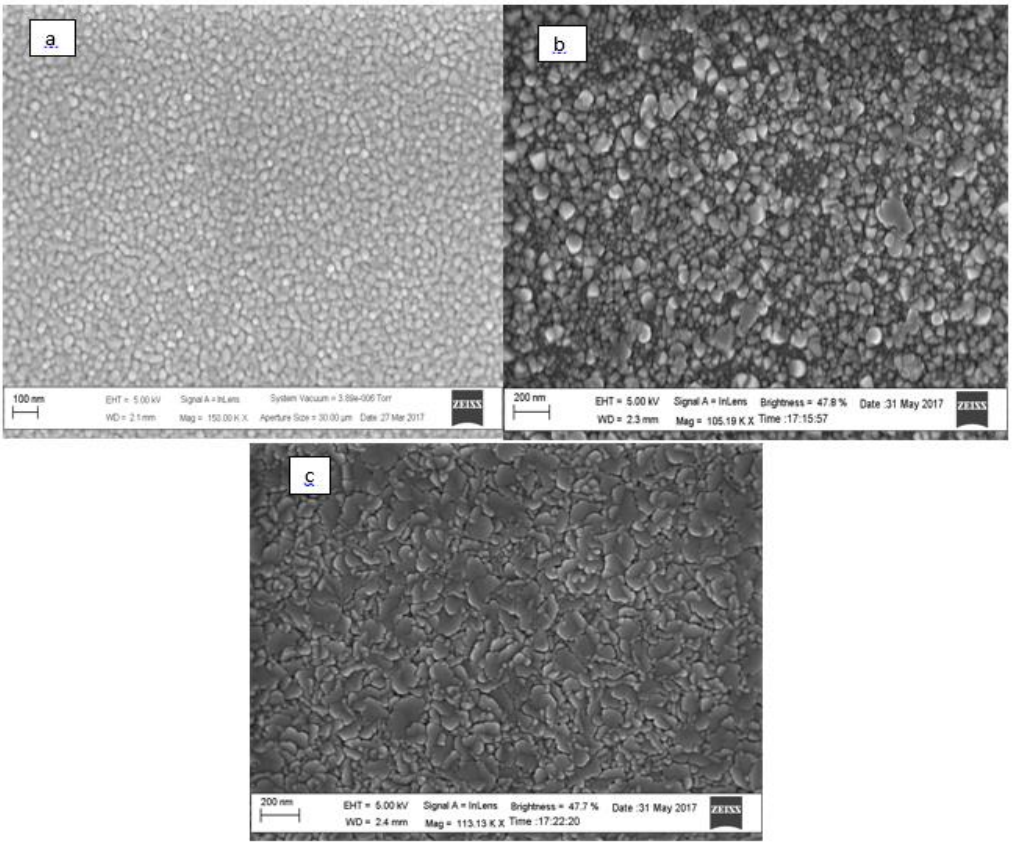

Fig.1. The SEM surface morphologies of WO_3 thin films deposited at different temperatures (a) 300 ℃, (b) 400 ℃ and (c) 500 ℃ respectively.

Figure 2 (a-c) shows the XRD (Cukα 1, $\lambda = 0.15406$ nm) spectra of the WO_3 thin films that were prepared by DC magnetron sputtering at different temperatures (300, 400 and 500 ℃). The X-ray diffraction patterns indicated by letters a, b and c are of the WO_3 thin films prepared at 300, 400 and 500 ℃ respectively and they show that WO_3 thin films obtained are highly crystalline. An increase of the crystalline quality can be envisaged by pattern of XRD spectra. The significant increase in the crystallinity quality could be attributed to the increase of deposition temperature.

The XRD pattern of WO_3 samples correspond to PDF card (01-071-0131), WO_3 deposited at different temperatures were identified to have an orthorhombic structure with units' cell lattice parameters of a = 7.341 Å, b = 7.570 Å, c = 7.754 Å and angle of 90º (for α, β and γ) and space group Pmnb (62). The strongest diffraction peak for all WO_3 films deposited appears at 2θ = 23º in (002) plane, indicating a fine preferential growth in the (002) direction. It was found that the deposition temperature also affects the crystallite size of the WO_3 nanoparticles. The crystallite size was calculated using Scherrer's formula [12] from the half width of the (002) peak for all WO_3 films and the results are tabulated in Table 1. It was observed that as the deposition temperature increases from 300 ºC to 500 ºC, the crystallite size also increased from 25 nm to 34 nm.

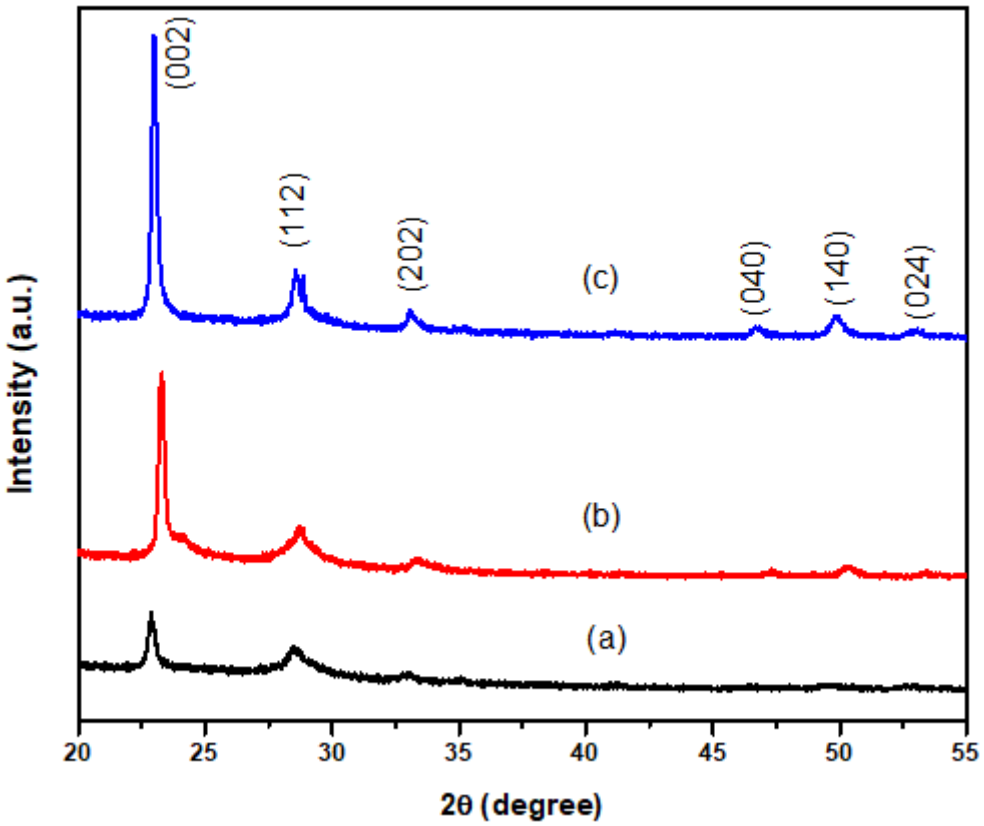

Fig. 2. The XRD patterns of WO_3 prepared by DC magnetron sputtering at different temperatures (a) 300 °C, (b) 400 °C and (c) 500 °C.

Table1. The crystallite size of WO_3 prepared by DC magnetron sputtering at different temperatures

Samples	Crystallite size (nm)
WO_3 – 300 °C	25
WO_3 – 400 °C	32
WO_3 – 500 °C	34

The samples were further characterized and analyzed for composition and thickness using RBS technique which was carried out using a beam of 3.6 MeV alpha particles ($^4He^{++}$). In Figure 3, 4 and 5 are the RBS spectra of 3.6 MeV ($^4He^{++}$) which was incident on the samples. It was observed from the RBS as indicated on Table 2 that the composition found is indeed WO_3 compound which agree with the XRD results. It was also observed from the RBS that the thickness of the samples deposited at different temperatures (300 ºC, 400 ºC and 500 ºC) were not the same. The thickness seemed to increase with an increase in the deposition temperature. The sample deposited at 300 ºC was found to have thickness of 120 nm, the sample deposited at 400 ºC was found to have a thickness of 360 nm. However, when compared with the sample deposited at 500 ºC, not much difference in thickness was observed since this sample was found to have a thickness of 370 nm. This increase in thickness might perhaps attributed by the increase in grain size or crystallite size of the samples as it was observed from the respective results of XRD. It should also be noted from SEM results that the morphology of the samples was not the same due to the change in deposition temperatures.

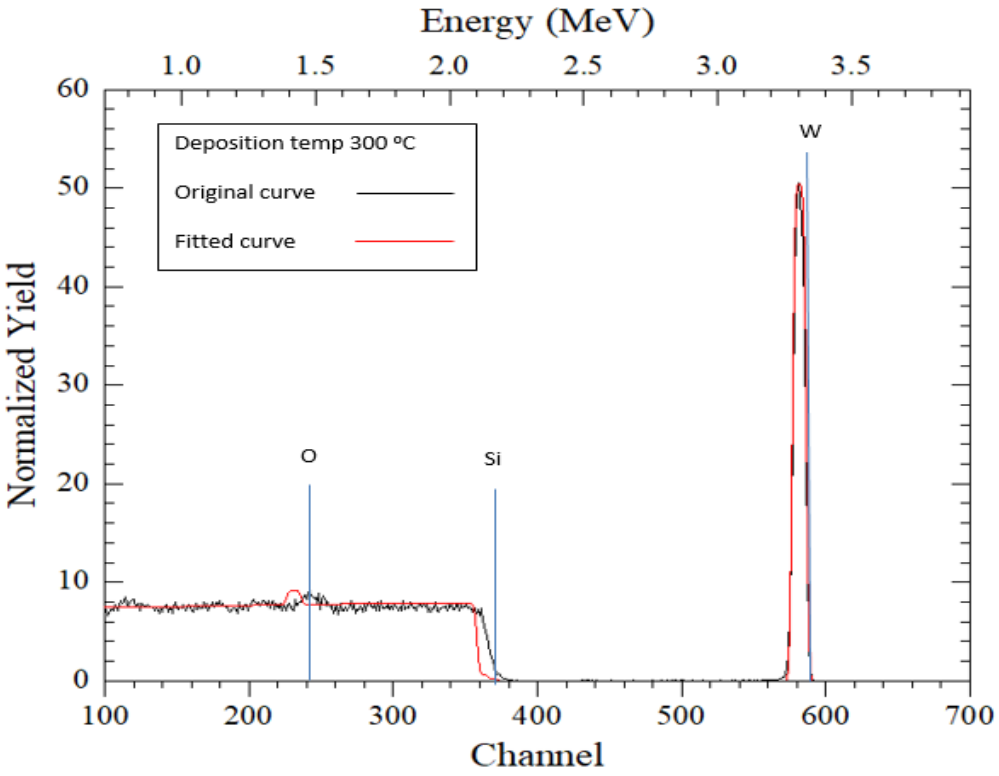

Fig. 3. RBS spectrum of 3.6 MeV ($^4He^{++}$) beam incident on WO_3 thin film deposited at 300 ºC by DC magnetron sputtering.

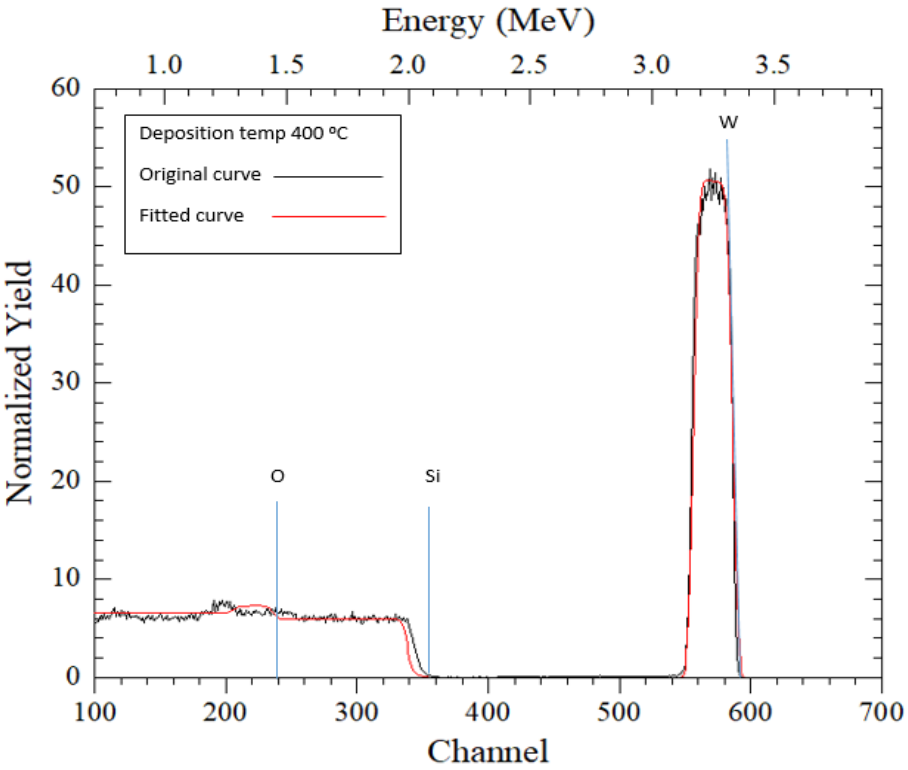

Fig. 4. RBS spectrum of 3.6 MeV ($^{4}He^{++}$) beam incident on WO_3 thin film deposited at 400 ºC by DC magnetron sputtering.

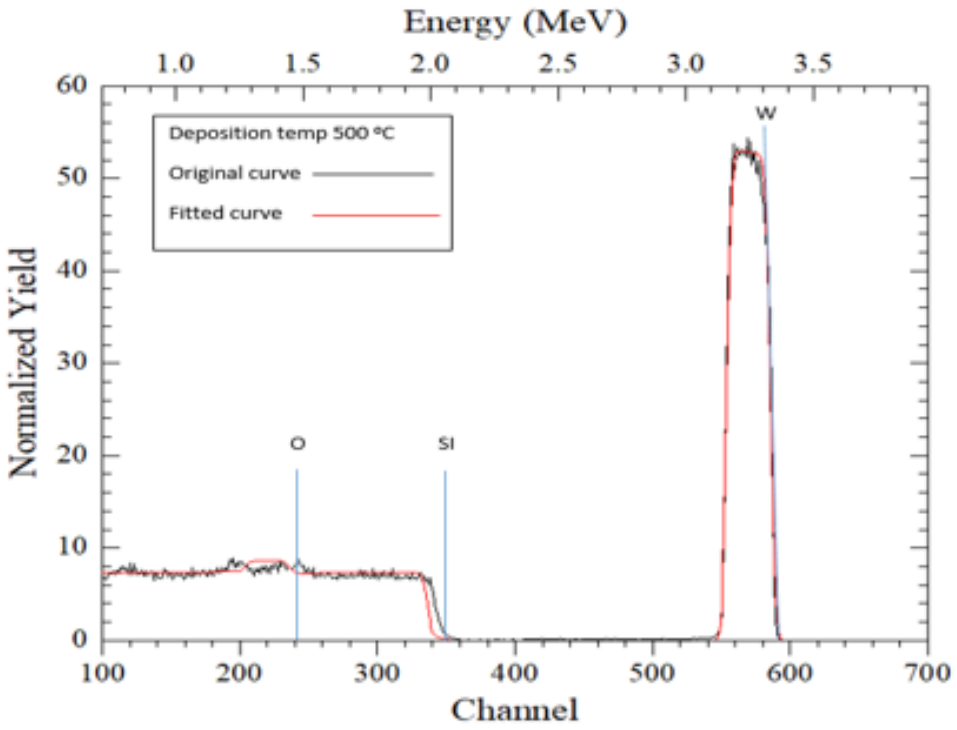

Fig.5. RBS spectrum of 3.6 MeV ($^{4}He^{++}$) beam incident on WO_3 thin film deposited at 500 ºC by DC magnetron sputtering.

Table 2. The composition and thickness of WO_3 prepared at different deposition temperatures

Samples	**Composition**		**Thickness (nm)**
WO_3 – 300 °C	W (27 %)	O (73%)	120
WO_3 – 400 °C	W (27%)	O (73%)	360
WO_3 – 500 °C	W (28%)	O (72 %)	370

Figure 6 shows the WO_3 based sensor film deposited on the alumina strip with platinum electrodes. The alumina strip was used because of its good electrodes for current flow and its melting point is high (melting point is 1768 ºC) [12]. Some previous studies [19] have shown WO_3 as a good sensor for NO_2 gas detection. However, in those studies high operating temperatures (above 200 ºC) were used during NO_2 detection to try to enhance the sensitivity of WO_3 based sensor and it has also been reported that WO_3 is not a good sensor at room temperature since it has high activation energy. Therefore, high operating temperature is required to enhance the sensitivity of WO_3 [20,21]. However, a good sensor of NO_2 which will be able to operate at room temperature is also needed since NO_2 can also be found at room temperature environment.

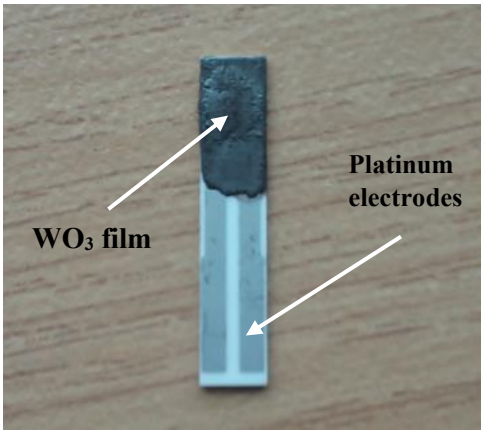

Fig. 6. The WO_3 based sensor film deposited at 500°C on the alumina strip having platinum electrodes.

WO_3 based sensors which were prepared at different deposition temperatures were each tested for their properties at room temperature on a gas sensing machine called Kenosistec at University of Zululand, but before testing the response of the sensors towards NO_2 gas, the sensors were first exposed into different relative humidity (RH%) to check their optimum humidity at room temperature. Figure 7 represents the response of the sensors towards 20 ppm NO_2 at room temperature at various relative humidity. It was observed that 70%RH is the optimum humidity for WO_3 based sensors and therefore the gas sensing properties of WO_3 based sensors were tested at 70%RH. It can be noted from Figure 7 that the humidity does affect the sensor response of WO_3 as NO_2 gas of 20 ppm is introduced to the surface of WO_3. It can also be seen that from 0%RH to 30%RH the sensor does respond towards the incoming NO_2 gas, but it does not show even a small recovery. However, the sensor started to show some recovery when the humidity was raised to 70%RH. At 90%RH the sensor did show some recovery however the response was negatively affected as it seems to drop when the humidity is above 70%RH, thus it can be concluded that the optimum humidity for WO_3 based sensor is 70%RH since the response and recovery of the sensors towards NO_2 gas was good.

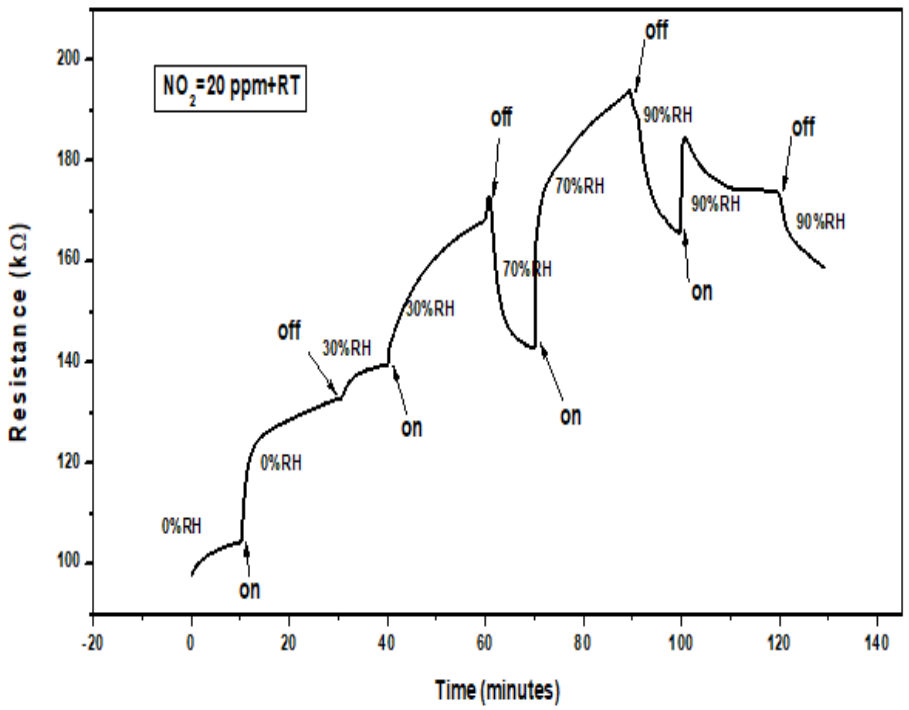

Fig. 7. The sensor response curve of WO_3 based sensor towards 20 ppm concentration of NO_2 gas at room temperature at different relative humidity.

When WO_3 based sensor film was exposed to the NO_2 gas, the resistance of the sensor increased to a certain value and then decreased to the original value once the NO_2 is switched off. This behavior is normal as reported in previous studies [11,12,17,19] since WO_3 is the n-type metal oxide semiconductor and NO_2 is the oxidizing gas. This type of behavior corresponds with gas sensing response of R_g/R_a where R_a is the resistance of the sensor, when no gas present on the sensor, and R_g is the resistance of the sensor when they are a gas introduced on the sensor. It shows the chemisorption of NO_2 to the WO_3 surface. Figure 8 shows the sensor response curve of the WO_3 metal oxide sensors deposited at 300 ºC, 400 ºC and 500 ºC. These sensors were exposed to different NO_2 concentrations at room temperature and at 70%RH. The NO_2 gas was switched on for 1200 seconds to check how fast the sensor is responding to the gas and switched off for 600 seconds to check how fast it is going to recover. It can be seen from Figure 8 that the sensors responded immediately to NO_2 gas at all concentrations, but they took some time to recover, and all of them appear not to be able to recover completely to their original resistance. However, the response and recovery time of the WO_3 based sensor appear to be slowly improving as the temperature was raised to 500 ºC and this can clearly be seen from Figure 10 where response and recovery time of each the sensor was calculated. Figure 9 shows the response curve of WO_3 based sensor deposited at 500 ºC. It can be noted from Figure 9 that when the relative humidity was still at 70%RH the sensor response of the sensor was good, but when it was raised to 90%RH during the detection of 150 ppm NO_2, the sensor response behavior changed, and this change shows that the sensor does not perform well at 90%RH. Figure 8 and Figure 9 shows that the initial resistance of WO_3 deposited at 500 ºC changed from starting at around 112 kΩ to start around 162 kΩ. This was attributed by the fluctuating factors during gas sensing e.g., humidity which was 70%RH±2%RH and the room temperature which was 17.6 ºC± 0.4 ºC.

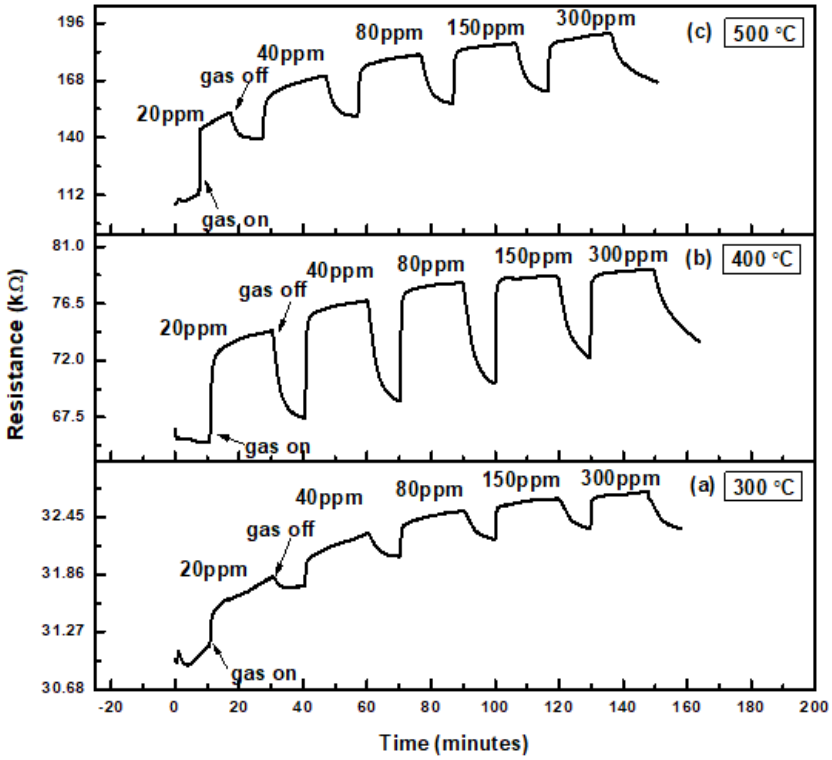

Fig. 8. WO_3 based sensor response curves for different NO_2 concentrations. The samples were grown at different deposition temperatures: (a) 300 ºC, (b) 400 ºC, and (c) 500 ºC.

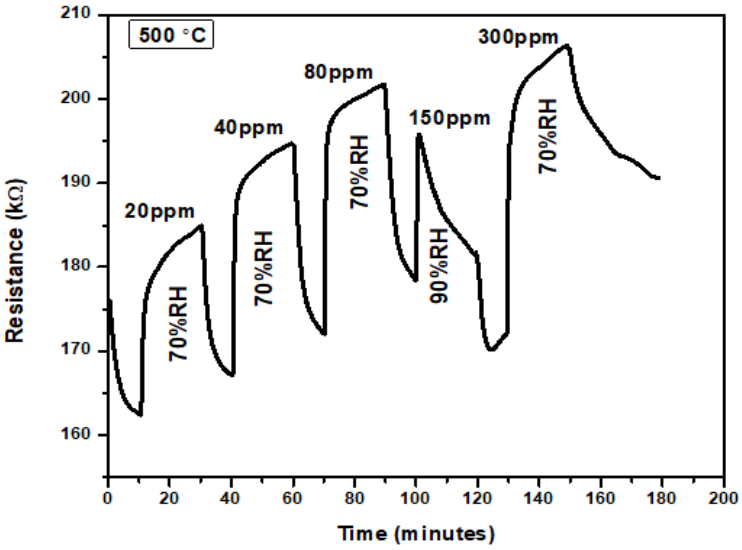

Fig 9. The response curve of WO_3 based sensor deposited at 500 ºC showing the effect of increasing humidity to 90%RH.

The response time and recovery time are one of the most important properties of the gas sensors because they indicate how fast the gas sensor will respond to the target gas and how fast does it recover to its initial resistance when the target gas has been switched on and thereafter switched off during testing in gas sensor machine. This is because the resistance of the sensor changes when it is exposed to the target gas and when it changes it shows that it is able to detect or sense that particular gas exposed to [1-17**]**. In Figure 10 the response and recovery time for gas sensors deposited at 300 ºC, 400 ºC and 500 ºC were calculated, the sensors were exposed to 80 ppm concentration of NO_2 at room temperature and 70%RH. It can be noted from Figure 10 that as the temperature which was used to prepare or deposit the WO_3 increased from 300 ºC to 500 ºC, the response and recovery time of WO_3 based sensor was improving. It was observed that the response time decreased from 142.2 to 108 seconds, and the recovery time decreased from 588.6 to 565.8 seconds. Therefore, it can be concluded from Figure 10 that WO_3 based sensor deposited at 500 ºC is a good sensor compared to those deposited at 300 ºC and 400 ºC, this also agree when comparing the sensitivity of the three sensors in Figure 11.

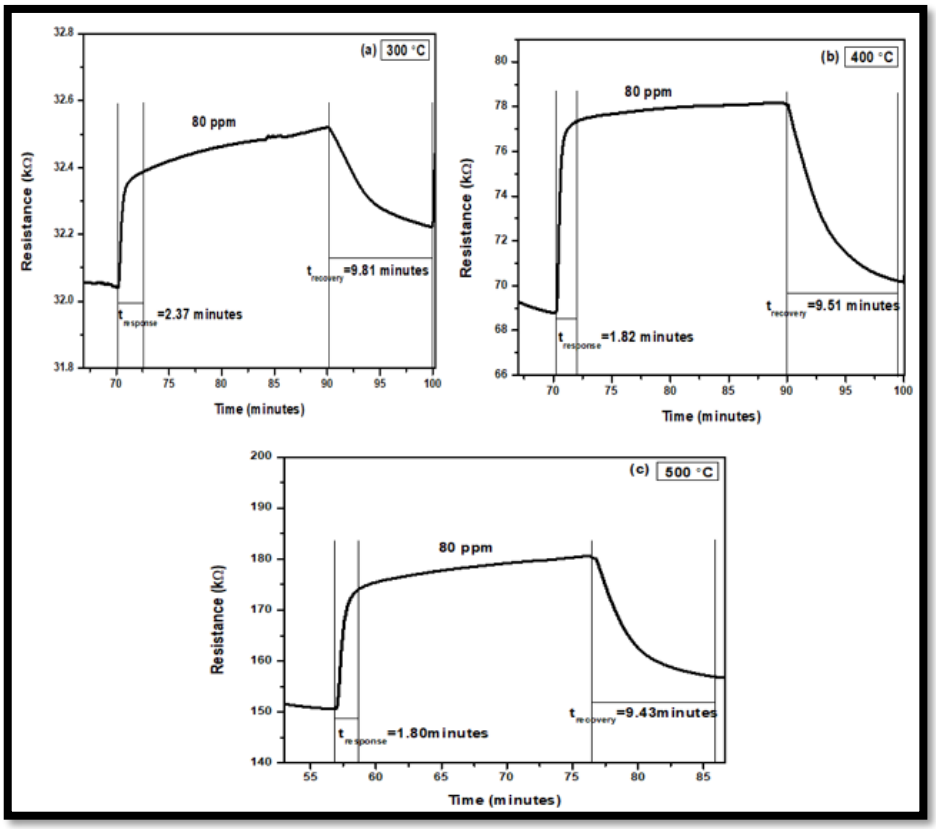

Fig. 10. The WO_3 sensor response curves, response, and recovery time ($t_{response}$ and $t_{recovery}$) of the sensors towards 80 ppm NO_2 at room temperature and 70%RH, deposition temperatures (300 ºC- 500 ºC).

The sensitivity is also the most important characteristic of the gas sensor because it tells us the rate at which the gas sensor responds towards the target gas, as the concentration of the gas increases [1-17,22,23]. The effectiveness of the gas sensor is determined by its sensitivity. The sensitivity ($\Delta S/\Delta C$) is determined from the slope of the linear curve of the sensor response (S) vs concentration (C). In Figure 11, the sensor response with concentration of NO_2 gas were plotted for different WO_3 based sensors deposited at different temperatures. It can be noted from Figure

12 that the sensitivity of WO_3 based sensor deposited at 500 ºC is a bit higher compared to other two sensors. The sensitivity was calculated from 80 ppm to 150 ppm for all three sensors. This is also true when looking at other concentrations (20 ppm to 40 ppm, 40 ppm to 80 ppm, and 150 ppm to 300 ppm) that the sensitivity of WO_3 deposited at 500 ºC is high compared to those deposited at 300 ºC and 400 ºC. Since WO_3 based sensor deposited at 500 ºC was the one to show good sensitivity, it was further tested to the varying NH_3 gas concentrations and to hydrogen gas at the same gas sensing environment (room temperature and 70%RH). It can be observed from Figure 12 that WO_3 based sensor did able to respond towards NH_3 gas, however the behavior of this sensing was not clear and the response towards this gas was not good compared to the response towards NO_2. In Figure 13 it can be observed also that WO_3 was not able to detect hydrogen gas even though the hydrogen concentrations were varied, this was perhaps occurring because NH_3 and H_2 are both reducing gases, hence WO_3 was selective to NO_2 gas.

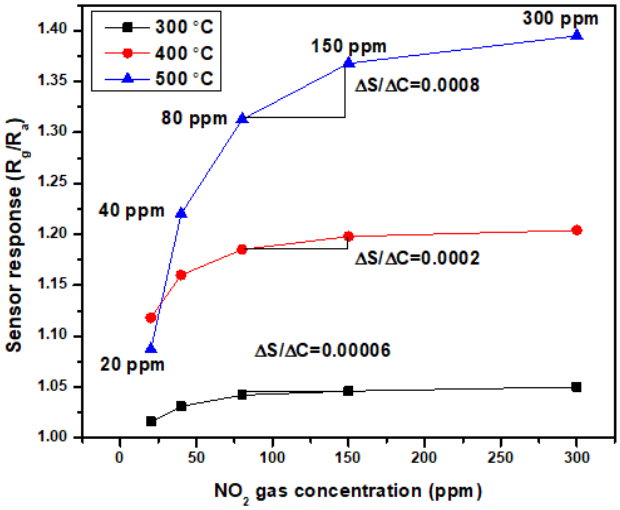

Fig. 11. The comparison of sensor response values and sensitivity of WO_3 based sensors of different deposition temperatures.

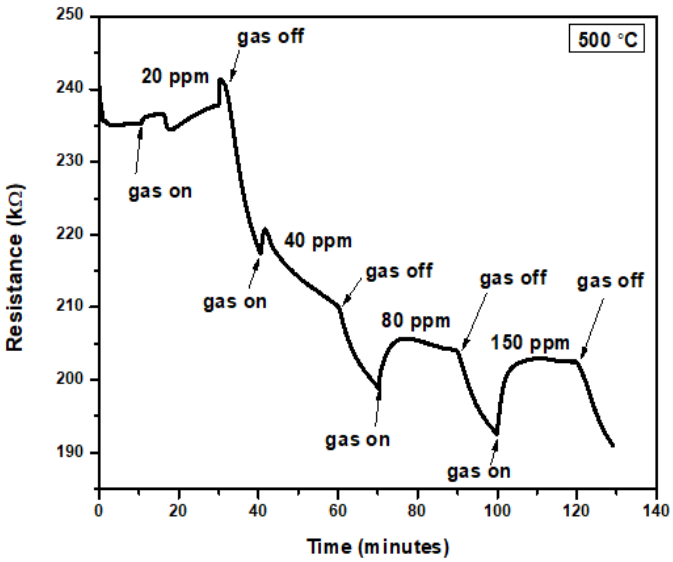

Fig. 12. The sensor response curve of WO_3 based sensor deposited at 500 ºC to the varying NH_3 concentrations.

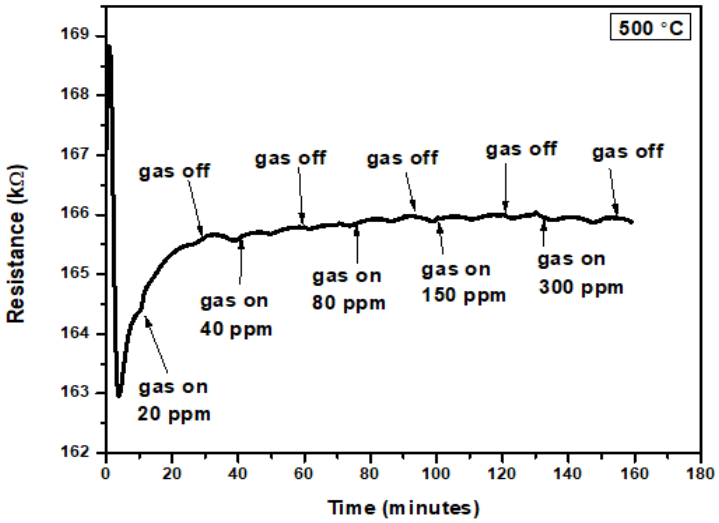

Fig. 13. The sensor response curve of WO_3 based sensor deposited at 500 ºC to the varying H_2 concentrations.

4. Conclusion

WO_3 nanostructured thin films were successfully deposited on alumina strips substrates using DC magnetron sputtering at different deposition temperature (300, 400 and 500 ºC). WO_3 thin films were characterized using XRD, SEM and RBS. From the XRD it was found that the samples (WO_3 thin films) were highly crystalline and that as the deposition temperature increases, the

samples become more crystalline, and this was observed since the diffraction peak intensity of the samples increased with the increase in deposition temperature. The increase in crystallite size of the samples with an increase in deposition temperature was also observed. From the SEM it was also found that the deposition temperature has more effect on the sample morphology since the morphology of the samples was completely different from each other. RBS confirmed that thin films of WO_3 were deposited on silicon and alumina strip substrates as indicated by the sample composition obtained from RBS which also agree with the XRD results. When increasing the deposition temperatures thickness of the samples also increases, this was thought as being attributed by the increase in grain size or crystallite size of the samples as this was observed from XRD results. The samples were tested on a gas-sensing machine (Kenosistec) for their gas sensing performance. It was found that the sample deposited at 500 ºC has a good gas sensing performance when compared to those that were deposited at 300 ºC and 400 ºC, and that it can be effectively used to sense NO_2 gas at room temperatures under the humidity of 70%RH. The NO_2 gas sensor based on WO_3 film deposited at 500 ºC showed the n-type behavior of sensing since the exposure to NO_2 gas resulted in the increase in its resistance, this is a normal behavior since NO_2 is an oxidizing gas and WO_3 is an n-type metal oxide. The WO_3 based sensor showed the poor response towards NH_3 and H_2 gases, which shows that WO_3 gas sensor is a selective to NO_2.

Acknowledgements

This work was financially supported by the NRF/DST, iThemba LABS and the research committee of the university of Zululand.

References

[1] Weiyi Zhang, Ming Hu, Xing Liu, Yulong Wei, Na Li, Yuxiang Qin. *Synthesis of the cactus-like silicon nanowires/tungsten oxide nanowires composite for room-temperature NO2 gas sensor*. Journal of Alloy and Compounds 679 (2016) 391-399.

[2] H. Zheng, J.Z. Ou, M.S. Strano, R.B. Kaner, A. Mitchell, K. Kalantar-zadeh. *Nanostructured tungsten oxide-properties, synthesis, and applications*. Adv. Funct. Mater. 21 (2011) 2175.

[3] S.K. Chong, C.F. Dee, S.A. Rahman. *Single reactor deposition of silicon/tungsten oxide core-shell heterostructure nanowires with controllable structure and optical properties*. RSC Adv. 5 (2015) 2346-2353.

[4] N. Lavanya, A.C. Anithaa, C. Sekar, K. Asokan, A. Bonavita, N. Donato, S.G. Leonardi, G. Neri. *Effect of gamma irradiation on structural, electrical and gas sensing properties of tungsten oxide nanoparticles*. Journal of Alloys and Compounds 693 (2017) 366-372.

[5] Lassner, Erik and Wolf-Dieter Schubert (1999). *Tungsten: properties, chemistry, technology of the element, alloys, and chemical compound*. New York: Kluwer Academic. ISBN 0-306-45053-4.

[6] Solleti Goutham, Sukhpreet Kaur, Kishor Kumar Sadasivuni, Jayanta Kumar Bal, Naradala Jayarambabu, Devarai Santhosh Kumar, Kalagadda Venkateswara Rao. *Nanostructured ZnO gas sensors obtained by green method and combustion technique*. Materials Science in Semiconductor Processing 57 (2017) 110-115.

[7] Ali Mirzaei, Gun-Joo Sun, Jae Kyung Lee, Chongmu Lee, Seungbok Choi, Hyoun Woo Kim. *Hydrogen sensing properties and mechanism of NiO-Nb2O5 composite nanoparticle-based electrical gas sensors.* Ceramics International (2017) 2-8.

[8] Martin S. Barbosa, Pedro H. Suman, Jae J. Kim, Harry L. Tuller, José A. Varela, Marcelo O. Orlandi. *Gas sensor properties of Ag- and Pd-decorated SnO micro-disks toNO2, H2and CO: Catalyst enhanced sensor response and selectivity.* Sensors and Actuators B 239 (2017) 253–261.

[9] Christopher S. Dandeneau, Yu-Hong Jeon, Christopher T. Shelton, Tom K. Plant, David P. Cann, Brady J. Gibbons. *Thin film chemical sensors based on p-CuO/n-ZnO heterocontacts.* Thin Solid Films 517 (2009) 4448–4454.

[10] J. Liang, W. Li, J. Liu, M. Hu. *Room temperature NO_2 sensing performance of free-standing mesh-structure vanadium dioxide nanorods by a chemical vapour deposition method*. Journal of Alloys and Compounds 687 (2016) 845-854.

[11] Z. Liu, T. Yamazaki, Y. Shen, T. Kikuta, N. Nakatani. *Influence of annealing on microstructure and NO2-sensing properties of sputtered WO3 thin films*. Sens. Actuators B 128 (2007) 173-178.

[12] Pi-Guey Su, Te-Tsun Pan. *Fabrication of a room-temperature NO2 gas sensor based on WO3 films and WO3/MWCNT nanocomposite films by combining polyol process with metalorganic decomposition method*. Materials Chemistry and Physics 125 (2011) 351–357.

[13] Angela I. Lopez-Lorente, Miguel Valcarcel. *The third way in analytical nanoscience and nanotechnology: Involvement of nanotools and nanoanalytes in the same analytical process*. Trends in Analytical Chemistry 75 (2016) 1-9.

[14] Gun-Joo Sun, Hyejoon Kheel, Jae Kyung Lee, Seungbok Choi, Sangmin Lee, Chongmu Lee. *H2S gas sensing properties of Fe2O3 nanoparticle-decorated NiO nanoplate sensors*. Surface and Coatings Technology 307 (2016) 1088-1095.

[15] Stanislav Haviar, Sarka Chlupova, Peterkus, Marcel Gillet, Vladimir Matolin, Iva Matolinova. *Micro-contacted self-assembled tungsten oxide nanorods for hydrogen gas sensing*. International Journal of Hydrogen Energy xxx (2016) 1-9.

[16] S.B. Upadhyay, R.K. Mishra, P.P. Sahay. *Cr-doped WO3 nanosheets: Structural, optical and formaldehyde sensing properties*. Ceramics International 42 (2016) 15301-15310.

[17] Engin Ciftyurek, Katarzyna Sabolsky, Edward M. Sabolsky. *Molybdenum and tungsten oxide based gas sensors for high temperature detection of environmentally hazardous sulfur species*. Sensors and Actuators B237 (2016) 262-274.

[18] D. Depla, S. Mahieu, J.E. Greene. *Sputter deposition processes*. (2010) 1-36.

[19] Derek R. Miller, Sheikh A. Akbar, Patricia A. Morris. *Nanoscale metal oxide-base heterojunctions for gas sensing: A review.* Sensors and Actuators B 204 (2014) 250-272.

[20] Y.G. Choi, G. Sakai, K. Shimanoe, N. Miura, N. Yamazoe, Sens. *Receptor Function and Response of Semiconductor Gas Sensor*. Actuators B 95 (2003) 258–265.

[21] T. Kida, A. Nishiyama, M. Yuasa, K. Shimanoe, N. Yamazoe. *Metal Oxide Semi-Conductor Gas Sensors in Environmental Monitoring*. Sens. Actuators B 135 (2009) 568–574.

[22] Dongzhi Zhang, Zhenling Wu, Peng Li, Xiaoqi Zong, Guokang Dong, Yong Zhang. *Facile fabrication of polyaniline/multi-walled carbonnanotubes/molybdenum disulfide ternary nanocomposite and its high-performance ammonia-sensing at room temperature*. Sensors and Actuators B 258 (2018) 895–905.

[23] Yuxiu Li, Dongyang Deng, Nan Chen, Xinxin Xing, Xu Liu, Xuechun Xiao, Yude Wang. *Pd nanoparticles composited SnO2 microspheres as sensing materials for gas sensors with enhanced hydrogen response performances*. Journal of Alloys and Compounds 710 (2017) 216-224.